



Published in final edited form as:

J Am Chem Soc. 2013 November 27; 135(47): . doi:10.1021/ja408230k.

Stilbene Vinyl Sulfonamides as Fluorogenic Sensors of and Traceless Covalent Kinetic Stabilizers of Transthyretin that Prevent Amyloidogenesis

Eul Hyun Suh^{1,2,*}, Yu Liu^{1,2,*}, Stephen Connelly^{3,4,*}, Joseph C. Genereux^{1,2,4}, Ian A. Wilson^{2,3}, and Jeffery W. Kelly^{1,2,4}

¹Department of Chemistry, The Scripps Research Institute, La Jolla, California, USA

²The Skaggs Institute for Chemical Biology, The Scripps Research Institute, La Jolla, California, USA

³Department of Integrative Structural and Computational Biology, The Scripps Research Institute, La Jolla, California, USA

⁴Department of Molecular and Experimental Medicine, The Scripps Research Institute, La Jolla, California, USA

Abstract

Small molecules that react selectively with a specific non-enzyme drug-target protein in a complex biological environment without displacement of a leaving group (tracelessly) are rare and highly desirable. Herein, we describe the development of a family of fluorogenic stilbene-based vinyl amides and sulfonamides that covalently modify transthyretin (TTR) tracelessly. These small molecules bind selectively to TTR in complex biological environments and then undergo a rapid and chemoselective 1,4-Michael addition with the pK_a-perturbed Lys-15 ε-amino group of TTR. Replacing the vinyl amide in **2** with the more reactive vinyl sulfonamide in **4** hastens conjugation kinetics. X-ray co-crystallography verifies formation of the secondary amine bond mediating conjugation in the case of **2** and **4** and confirms the expected orientation of the stilbene within the TTR binding sites. Vinyl amide **2** and sulfonamide **4** potently inhibit TTR dissociation and amyloid fibril formation *in vitro*. The TTR binding selectivity, modification yield, and reaction chemoselectivity of vinyl sulfonamide **4** is good enough in human plasma to serve as a starting point for medicinal chemistry efforts. Moreover, vinyl sulfonamide **4** is fluorogenic, i.e. it exhibits minimal background fluorescence in complex biological environments, remains dark upon binding to TTR, and only becomes fluorescent upon reaction with TTR. The fluorogenicity of **4** was utilized to accurately quantify the native TTR concentration in *E. coli* lysate using a fluorescence plate reader.

INTRODUCTION

Transthyretin (TTR) is one of more than 30 human proteins that are known to misfold and/or misassemble into pathology-associated aggregates, possibly including cross-β-sheet amyloid fibrils.^{1–5} Compelling pharmacologic, surgically mediated gene therapy, and human genetic

Correspondence should be addressed to J.W.K. (jkelly@scripps.edu).

*These authors contributed equally

The authors declare no competing financial interests.

Supporting information. Figures S1–S13. Table S1. Supporting experimental methods. This information is available free of charge via the internet at <http://pubs.acs.org>.

evidence indicates that the process of TTR aggregation causes post-mitotic tissue loss characteristic of the TTR amyloid diseases (amyloidoses).^{6–15} Rate-limiting tetramer dissociation and monomer misfolding enable TTR aggregation.^{10,11,16–18}

Small molecules that bind to one or both of the unoccupied thyroxine (T₄)-binding sites within the TTR dimer-dimer interface bisected by the crystallographic 2-fold axis (C₂) (Figure 1; bound T₄ is shown) preferentially stabilize the native tetrameric structure of TTR over the dissociative transition state, increasing the kinetic barrier for tetramer dissociation.^{11,19,20} These so-called kinetic stabilizers dramatically slow TTR dissociation and aggregation,^{11,21} and a clinical trial with one of them, tafamidis, in V30M-TTR-linked familial amyloid polyneuropathy patients demonstrates significant and sustained slowing of autonomic and peripheral neuropathy progression relative to placebo.^{8,9}

Previously, we reported covalent kinetic stabilizers that selectively bind to the TTR T₄-binding sites and then rapidly and chemoselectively react with the pK_a-perturbed Lys-15 ε-amino group at the periphery of the binding sites.^{22–24} These covalent TTR kinetic stabilizers are appealing drug candidates because lower concentrations can often be employed relative to non-covalent kinetic stabilizers.²⁵ To produce the previously published TTR covalent kinetic stabilizers, non-covalent TTR kinetic stabilizers were re-engineered to harbor a reactive ester, a thioester, or a sulfonyl fluoride substituent.^{22–24} These electrophiles liberate phenol, thiophenol or a fluoride ion, respectively, as leaving groups upon nucleophilic attack by the Lys-15 ε-amino group of TTR when forming their conjugates. The liberation of a leaving group into the human body could present an undesirable toxicity risk for diseases requiring life-long treatment, like the TTR amyloidoses. Thus, a traceless covalent kinetic stabilizer of TTR would be a welcome addition to the list of drug candidates to ameliorate the TTR amyloidoses.

Herein, we describe our efforts to produce traceless small molecule covalent kinetic stabilizers of TTR, utilizing stilbene-based vinyl amides and sulfonamides (Table 1) conceived of by structure-based design principles as a starting point.^{26–31} Stilbene-based vinyl amides and sulfonamides bind to TTR and then undergo a rapid and chemoselective 1,4-Michael addition with the Lys-15 ε-amino group of TTR, affording a secondary amine linkage between TTR and the stilbene substructure (confirmed by x-ray crystallography) in the absence of leaving group displacement. The TTR binding selectivity, modification yield, and reaction chemoselectivity of vinyl sulfonamide **4** in human plasma is good enough for it to serve as a medicinal chemistry starting point to develop a TTR amyloid disease ameliorating drug, especially considering its efficacy as a TTR amyloidogenesis inhibitor or kinetic stabilizer *in vitro*.

Moreover, vinyl sulfonamide **4**, upon reacting with TTR affords a conjugate that is fluorescent in *E. coli* lysate, wherein **4** remains dark in this complex biological sample before reacting with TTR. This fluorescent conjugate exhibits a quantum yield that is four-fold higher than previously reported TTR fluorescent conjugates. Taking advantage of the fluorogenicity of **4**, we quantified the amount of native TTR in *E. coli* lysate using a fluorescence plate reader.

EXPERIMENTAL METHODS

RP-HPLC analysis of TTR modification by compounds 1–4

WT-TTR and K15ATTR were expressed in *E. coli* and purified as described previously.³² Compounds **1–4** at the indicated concentrations were mixed with WT-TTR or K15A-TTR (3.6 μM; 0.2 mg/mL) in 500 μL of 10 mM sodium phosphate buffer (pH 7.0) with 100 mM KCl, and 1 mM EDTA added (hereafter referred to as PBS buffer) and these candidate

kinetic stabilizers were incubated for 10 min, 18 h, or 24 h at 37 °C. The reaction mixture was subjected to reverse phase high performance liquid chromatography (RP-HPLC) on a Waters 600E multi-solvent delivery system, using a Waters 486 tunable absorbance detector, a 717 autosampler, and a Thermo Hypersil Keystone Betabasic-18 column (50 mm, 150 Å pore size, 3 µm particle size). Mobile phase "A" comprises 0.1% TFA in 94.9% H₂O + 5% CH₃CN and mobile phase "B" is made up of 0.1% TFA in 94.9% CH₃CN + 5% H₂O. A linear gradient from 0 to 100% B over 50 min at a flow-rate of 1 mL/min was used to generate the chromatogram. For kinetic analysis of conjugate formation between TTR and compound **2** or **4**, WT-TTR (3.6 µM) was incubated with compound **2** or **4** at a concentration of 3.6 µM or 7.2 µM for the indicated times at 37 °C and the reaction mixture was subjected to RP-HPLC as described above.

Transthyretin fibril formation in the presence of the test compounds

A candidate kinetic stabilizer (5 µL of a 1.44 mM, 0.72 mM, 0.36 mM, 0.18 mM, 0.09 mM, or 0.045 mM solution in DMSO) was mixed with 495 µL of WT-TTR (7.2 µM) in PBS buffer and incubated for 10 min at 37 °C. 500 µL of 100 mM acetate buffer (pH 4.2) containing 100 mM KCl and 1 mM EDTA was added to the reaction mixture to obtain final pH of 4.4. The mixture was incubated for 72 h without agitation at 37 °C. Turbidity of the reaction mixture was measured at 400 nm using a UV spectrophotometer after briefly vortexing the sample to evenly distribute any precipitates. For kinetic analysis of fibril formation of TTR in the presence of test compounds, turbidity was measured at the indicated time points after vortexing.

Measuring the kinetics of transthyretin tetramer dissociation

Two hundred µL of WT-TTR (18 µM) in PBS buffer was incubated with compound (**2**, **4**, or **6**) at 18 µM (TTR : covalent kinetic stabilizer = 1 : 1) or 36 µM (TTR : covalent kinetic stabilizer = 1 : 2) for 10 min or 18 h at 37 °C. The reaction mixture (100 µL) was mixed with 900 µL of a 6.67 M urea solution in PBS buffer (final urea concentration = 6 M; under these conditions TTR refolding and reassembly are not possible). The mixture was incubated in the dark without agitation at 25 °C and circular dichroism (CD) spectra were measured at 215–218 nm (scanned 5 times at every 0.5 nm with 10 sec averaging time) at the indicated time points.

Evaluating transthyretin conjugate fluorescence

Compound **2** or **4**, 5 µL of 0.72 mM or 0.36 mM solution in DMSO, was mixed with 500 µL of WT-TTR or K15A-TTR homotetramer (0.2 mg/mL, 3.6 µM) in PBS buffer and incubated at 37 °C for 30 min (compound **4**) or 18 h (compound **2**) (final concentration of covalent kinetic stabilizers: 7.2 µM or 3.6 µM). The fluorescence changes were monitored in a Varian Cary 50 spectrofluorometer using a 1-cm path length quartz cuvette at 37 °C. The excitation slit was set at 5 nm and the emission slit was set at 10 nm. The PMT was set to 500 V for compound **4** and 550 V for compound **2**. The samples were excited at 327 nm, and the emission spectra were collected from 340 to 550 nm. For the kinetic analysis of conjugation of compound **4** (3.6 µM or 7.2 µM) to WT-TTR (3.6 µM), fluorescence emission at 395 nm was measured every 10 sec for 30 min at 37 °C.

Quantum yield measurement

Compounds **4** and **5** (7.2 µM) alone in either benzene or in PBS buffer, or together with WT-TTR (3.6 µM) in PBS buffer were incubated overnight at 25 °C before measuring the quantum yields. Quantum yields were measured following previously published methods.²⁴ Quinine bisulfate in 0.5 M H₂SO₄ was used as a reference ($\Phi_{\text{ref}} = 0.546$).

Modification of TTR in human plasma by compound 4

The modification ratio of WT-TTR in human plasma by compound 4 was evaluated using a combination of quantitative immunoblotting and RP-HPLC employing fluorescence conjugate detection. A human plasma sample was centrifuged at 16,000 g for 5 min at 4°C to remove particulates. To quantify the total TTR concentration in the sample using quantitative immunoblotting, 20 µL plasma was denatured in 20 µL 2X SDS loading buffer for 5 min at 95 °C. The sample was further diluted 10 fold or 20 fold using 1X SDS loading buffer to avoid saturation of signal. A standard curve of recombinant WT-TTR was also prepared. Samples (5 µL) were loaded on a 4–20% SDS-gradient gel and run in Tris-glycine running buffer. TTR was detected using a monoclonal mouse antibody against TTR (produced by The Scripps Research Institute's Antibody Production Core Facility). To quantify labeled TTR in plasma, the same plasma sample was incubated with either 20 or 40 µM 4 at 37°C for 30 min. The samples were analyzed by RP-HPLC as described above using a linear gradient from 0 to 100% B over 60 min at a flow-rate of 1 mL/min. The fluorescence detector was set at an excitation wavelength of 327 nm and an emission wavelength of 395 nm.

Assessing k_{chem} and K_i of TTR conjugate formation using fluorescence

Compound 4 (0.2 µM) was added to increasing concentrations of WT-TTR in PBS buffer at 25 °C being mindful that 1 µM WT-TTR tetramer is equivalent to 2 µM of TTR binding pockets. The fluorescence time course was recorded using an excitation wavelength of 327 nm and an emission wavelength of 395 nm. The emergence of conjugate fluorescence followed single turn-over pseudo-first order reaction kinetics at different concentrations of TTR binding pockets, which allowed for calculation of the observed rate constant (k_{obsd}) at each TTR binding pocket concentration. Individual k_{obsd} at the different concentrations were then fitted into the equation:

$$k_{\text{obsd}} = k_{\text{chem}} \cdot [\text{compound 4}] / (K_i + [\text{compound 4}])$$

k_{chem} is the maximum rate constant of the chemical labeling step of Michael addition that is achieved at an infinite concentration of compound 4. K_i defines the concentration of compound 4 that yields a half maximal rate of conjugation.

Quantification of tetrameric TTR in *E. coli* lysate by fluorescence

Resuspended K12 *E. coli* cells were lysed by sonication on ice (with two 30 sec sonication pulses, each followed by with 60 sec pauses to re-establish a lower temperature), then centrifuged at 16,000 g for 30 min at 4°C. The resulting supernatant was collected as the soluble fraction for subsequent analysis. Indicated concentrations (0 µM, 0.9 µM, 1.8 µM, 3.6 µM, 7.2 µM) of tetrameric TTR were prepared by diluting a stock solution of recombinant TTR (36 µM tetramer) into the *E. coli* lysate. Compound 4 (20 µM or 30 µM) was then added to the TTR and the labeling kinetics were monitored by fluorescence in a Molecular Devices SpectraMax plate reader using an excitation wavelength of 327 nm and an emission wavelength of 395 nm. The amount of TTR added to *E. coli* lysate generated a standard curve that was identical to the standard curve generated from TTR in PBS buffer based on the final fluorescence intensity. The time courses of the fluorescence increases were effectively identical as well, except for the highest TTR concentration added to *E. coli* lysate.

RESULTS AND DISCUSSION

Using a Stilbene-based Vinyl Amide to Label TTR Covalently

To develop a traceless covalent TTR kinetic stabilizer, we employed the substituted stilbene structure conceived of by structure-based design that nicely complements the structure of the T₄-binding sites within the TTR tetramer.^{28,29} Since the vinyl amide was envisioned to have intrinsic chemical reactivity towards the pK_a-perturbed Lys-15 ε-amino group of TTR, via a Michael addition mechanism, we attached this functional group to the stilbene backbone. The stilbene-based covalent kinetic stabilizer **1** (Table 1), harboring a *meta* vinyl amide functional group relative to the *trans* double bond, was envisioned to have the proper geometry to allow the Lys-15 pK_a-perturbed ε-amino group of TTR to attack the antibonding orbitals of the terminal *sp*² hybridized carbon. Multiple vinyl amide-based covalent drug candidates are in clinical trials and have been demonstrated to be potent and selective inhibitors in cells; thus, these have potential as traceless covalent TTR kinetic stabilizers.²⁵

We evaluated whether stilbene **1** (Table 1) could covalently label recombinant WT-TTR in PBS buffer, as ascertained by reverse phase high performance liquid chromatography (RP-HPLC) and by LC-ESI mass spectrometry (LC-ESI-MS) analysis. Surprisingly, no covalent modification was observed, shown both by the recovery of **1** and the appropriate quantity of unmodified WT-TTR subunits (Figure S1a), and by only the unlabeled TTR subunit mass peak being detected (Figure S1b).

We next evaluated whether the *para*-substituted analogue **2** (Table 1) could label TTR in PBS buffer (*in vitro*). By RP-HPLC, an additional TTR subunit peak was observed besides the unmodified TTR subunit peak and only a small quantity of unreacted **2** was recovered after a 18 h incubation period, suggesting covalent modification of WT-TTR by **2** (Figure 2a). Covalent modification of the TTR subunit by **2** was further confirmed by the observation of an additional LC-ESI mass signal corresponding to the mass of the TTR-**2** secondary amine conjugate (Figure 2b). To explore whether **2** primarily modified the pK_a-perturbed Lys-15 residue of TTR, we evaluated the chemoselectivity of **2** towards K15A-TTR in PBS buffer, a TTR mutant in which Lys-15 is replaced with Ala. No modified TTR subunit peak was observed (Figure 2c) and nearly all of the unreacted **2** was recovered, further confirming the lack of modification. We attempted to identify the composition of the small peak in Figure 2a at the longest retention time, unsuccessfully—it may be a TTR subunit modified by **2** at both Lys15 and Cys10.

The kinetics of the reaction between WT-TTR and **2** was estimated by monitoring the increasing intensity of the covalent conjugate HPLC peak as a function of time (Figure 2d). Conjugate formation utilizing vinyl amide **2** was relatively slow, exhibiting a covalent modification half time (*t*_{1/2}) based on an exponential fit to the data of 5.3 h at a reaction stoichiometry of 2:1 (compound **2** to TTR). Complete modification was only observed after 24 h.

We hypothesized that faster kinetics could be achieved by enhancing the reactivity of the electrophile. We attempted to enhance the reactivity of the *para* vinyl amide substituent by introducing an electron withdrawing chlorine atom on the terminal *sp*² hybridized carbon atom, leading to vinyl amide **3** (Table 1). Surprisingly, compound **3** did not react with WT-TTR as demonstrated by RP-HPLC (Figure S2), possibly due to steric hindrance associated with introduction of the chlorine atom.

Vinyl Sulfonamides as Electrophiles to Covalently and Chemoselectively React with TTR with Improved Efficiency and Enhanced Kinetics *in vitro*

To enhance the reactivity of the Michael acceptor, we replaced the *para* vinyl amide substituent in **2** by the more reactive *para* vinyl sulfonamide of **4** (Table 1). The sulfonamide exhibits a stronger electron withdrawing effect than the secondary amide comprising **2**.³³ We first asked whether **4** was able to label WT-TTR in PBS buffer. Nearly complete covalent modification of WT-TTR (3.6 μM) was achieved by reaction with **4** (3.6 or 7.2 μM) after only a 10 min incubation period at 37°C, as discerned by RP-HPLC analysis (Figure 3a). The TTR-**4** conjugate yields, reflecting labeling efficiency, were calculated from the remaining unmodified TTR subunits as 24.7% and 46% at a concentration of 3.6 and 7.2 μM **4**, respectively, after a 10 min incubation period (25 and 50 % being maximal, reflecting conjugation to one or two TTR subunits comprising the TTR tetramer, respectively). In addition, LC-ESI-MS analysis demonstrated that approximately 50% of TTR subunits were modified by **4**, as shown by the relative intensities of the modified and unmodified peaks on the LC-ESI-MS trace at a TTR to compound **4** stoichiometry of 1:2 (3.6 μM TTR and 7.2 μM **4**) (Figure 3b). Thus, **4** labels WT-TTR fast and efficiently, affording a product of the expected mass.

An HPLC-based time course of conjugate formation confirms the rapid 1,4 addition kinetics of **4** to WT-TTR (Figure 3c). The time to 50% completion ($t_{1/2}$) based on an exponential fit to the data was estimated to be 69 sec, with complete labeling being observed in less than 5 min, 270 times faster than the conjugation kinetics of **2** ($t_{1/2}$ = 5.3 h, complete labeling at 24 h). Increasing the reactivity of the Michael acceptor dramatically increases the rate of conjugate formation.

The chemoselectivity of WT-TTR conjugate formation by **4** *in vitro* was demonstrated using K15A-TTR. That the pK_a -perturbed Lys-15 ϵ -amino group of WT-TTR was modified by **4** is reflected by the lack of TTR modification when the K15A-TTR homotetramer was reacted with **4**, according to RP-HPLC analysis (Figure S3). We recovered 100% of **4** that we started with, indicating no off-target labeling by **4** over the period wherein WT-TTR is 92% labeled by **4**. Further validation of chemoselectivity derives from the observation that no modification was observed when monomeric TTR (m-TTR)³⁴ was incubated with **4** over a 24 h period by LC-ESI-MS, indicating that **4** only modifies the pK_a perturbed Lys-15 residue in the T₄ binding site of the properly folded TTR tetramer (Figure S4). Direct evidence of Lys-15 ϵ -amino modification by **4** in WT-TTR was demonstrated by LC-MS-MS data (Figure S5). We observed no modification other than at Lys-15 at a TTR to compound **4** stoichiometry of 1:2 (3.6 μM TTR and 7.2 μM **4**) over a 24 h reaction period (Figures S5a and b). We further probed the chemoselectivity of **4** by incubating with an excess amount of **4** for 24 h (23 h and 50 min longer than the period required to achieve maximal conjugation). Incubation at a TTR to compound **4** stoichiometry of 1:3 (3.6 μM TTR and 10.8 μM **4**) before processing for LC-MS-MS led to some off-target modification of the Cys-10 residue as expected, due to the intrinsic reactivity of **4** towards a thiol group (Figures S5c and d). Importantly, this modification was not observed with K15A-TTR (Figure S3), suggesting Cys-10 was only activated for modification after accommodation of **4** in the binding pocket. Therefore, the additional modification of Cys-10 could only be observed when an excess amount of **4** was used and the Cys-10 labeling is very slow compared to Lys-15 labeling.

Thus, we have demonstrated that **4** is a very fast and efficient covalent modifier of WT-TTR and is chemoselective towards Lys-15 if the incubation time and stoichiometry are properly controlled *in vitro*. Off-target labeling of Cys-10 residue is not a concern given that complete labeling of Lys-15 occurs within a period of 10 min.

Crystallographic Analysis of WT-TTR-(Kinetic Stabilizer)₂ Conjugates

A crystal structure of the non-covalent complex between **1** and WT TTR, as well as the conjugates resulting from the reaction between WT-TTR and compounds **2** and **4** were determined at 1.33, 1.45, and 1.22 Å resolution, respectively (Figures 4a–c; see Table S1 for data collection and refinement statistics). In all of the structures, the previously optimized 3,4-dimethyl-4-hydroxyphenyl substructure occupies the inner binding subsite, with the 3,5-dimethyl substituents projecting into halogen binding pockets (HBPs) 3 and 3' while the 4-hydroxy group engages in hydrogen bonding with the Ser117/117' residues at the base of the T₄-binding pocket, bridging adjacent TTR subunits. The second aryl ring occupies the binding site area between HBP1 and 1'. While the density identifying the secondary amine tether in the unbiased 2Fo-Fc electron density maps was clear for **2**, the analogous substructure originating from **4** had more diffuse electron density in the outer binding subsite, owing to at least two major conformations afforded by rotation about the aryl sulfonamide bond (Figure S6). Sulfonamides are less rigid than their amide counterparts resulting in more accessible conformations. The pyramidal N atom of the sulfonamide substructure contrasts with the planar NH in an amide bond. The torsion angle ω ($\angle C^{\alpha}SNC^{\alpha}$) minima of the sulfonamide bond range from -100° to $+60^{\circ}$, in contrast to the familiar values of 180° for a *trans*- and 0° for a *cis*-secondary amide bond. Lastly, the energy barriers for rotation around the S-N bond are lower than for the C-N bond (30–40 kJ/mol vs. 60–90 kJ/mol, respectively). In order to maintain good bond angle geometry and bond lengths within the sulfonamide derived from conjugate formation between TTR and **4**, the bond length and angle restraints were further increased in this more disordered region around the incident 2-fold axis during refinement.

In the case of the previously reported ester, thioester (e.g. **6**; Table 1) and sulfonyl fluoride (e.g. **7**; Table 1) substituted covalent kinetic stabilizers of TTR, positioning the reactive group in the *meta* position of the ring occupying the outer binding site was optimal for chemoselective reaction with Lys-15 of TTR;^{22–24,35} however, placing the vinyl amide or sulfonamide group in the *meta* position resulted in very poor reaction kinetics, as described above.

Increasing the reactivity of the electrophile, i.e. in going from **2** to **4**, must be thoughtfully managed to avoid a decrease in TTR modification selectivity in the context of complex biological samples. To maximize the selectivity of TTR conjugate formation using vinylsulfonamides, both their binding must be high affinity and their subsequent reaction kinetics must be fast. While structure-based design can lead to aromatic vinylsulfonamides with a high complementarity to the TTR binding sites and thus afford a higher fraction of molecules that will bind with high affinity, predicting their desolvation energies and thus their binding constants is extremely difficult and thus there is no substitute for making a lot of analogs and experimentally measuring K_i values (see below; binding is a component of this term) to optimize binding. In other words, structure-based design is not a substitute for a traditional structure activity relationship study to optimize K_i , which was not done in this paper.

While structure-based design cannot predict good binders *a priori*, this approach is more reliable for making predictions about where to place the vinylsulfonamide substituent to achieve a maximum rate of conjugation (k_{chem} ; see below) post-binding. It is clear from the structure of **1** bound to TTR that placing a vinylamide and very likely the vinylsulfonamide group in the *meta*-position precludes the ϵ -amino group from engaging with the antibonding orbital of the alkene terminal carbon—an interaction which is necessary for the conjugation reaction to occur. Moving the vinylamide or the vinylsulfonamide substituent to the *para* position allows the low energy extended conformation of the Lys side chain to make a

energetically accessible approach to the antibonding orbital of the terminal sp^2 hybridized carbon atom. In summary, structure-based design is good at predicting ligand binding orientation and the relative positioning of the electrophile and the nucleophile and thus the propensity for the conjugation reaction to occur, but it is not good at predicting binding selectivity, because desolvation energies and binding to competitor proteins are hard to predict a priori.

Inhibiting Acid-mediated TTR Amyloid Fibril Formation by Covalent Kinetic Stabilization

We next investigated the ability of the WT-TTR conjugates, derived from reactions between vinyl amide **2** or vinyl sulfonamide **4** with WT-TTR, to misfold and aggregate (undergo amyloidogenesis) under previously established acid-mediated fibril formation conditions.³⁶ Preincubation of **2** or **4**, or the previously reported thioester-based covalent stabilizer **6** (Table 1) with TTR (3.6 μM) for 10 min at a range of concentrations (0 – 7.2 μM) before increasing the denaturation and aggregation stress by decreasing the pH to 4.4 reveals a near maximal inhibition of fibril formation after a 120 h aggregation period at a covalent kinetic stabilizer concentration of 3.6 μM (Figure 5a). This is consistent with previous reports that occupancy of one of the two T_4 -binding sites within TTR is sufficient to kinetically stabilize the entire tetramer and inhibit amyloidogenesis.²⁰ Examination of the time course of acid-mediated TTR (3.6 μM) fibril formation (pH 4.4, 37 °C) as a function of the concentration of **4** (2.7, 3.6 or 7.2 μM) reveals substantial dose-dependent inhibition of WT-TTR amyloidogenesis (Figure 5b and Table 2). Previous studies demonstrate that measuring the rate of TTR aggregation by Thioflavin T fluorescence or by turbidity affords different curve shapes, especially early in the aggregation reaction, however for the purposes of looking at inhibition over a period of 72 h, both approaches are sufficient and equivalent.³⁷

Inhibition of WT-TTR Dissociation by Covalent Kinetic Stabilizers **2** and **4**

The slowing of the rate of urea-induced WT-TTR dissociation (and subsequent denaturation) owing to conjugate formation between WT-TTR and **2** and **4** was assessed. Since conjugate formation renders the dissociation barrier of WT-TTR largely insurmountable under physiological conditions, urea was added to accelerate dissociation.^{22,24} Recombinant WT-TTR (1.8 μM) was pre-incubated for 10 min with **2**, **4**, or **6** as a function of their concentration (1.8 or 3.6 μM) to subsequently study dissociation kinetics over a 168 h timescale (Figure 5c).¹⁸ Far-UV CD enabled monitoring the kinetics of linked TTR tetramer dissociation and monomer denaturation (fast relative to dissociation), hastened by the presence of 6 M urea, which prevents monomer refolding and thus renders dissociation irreversible.¹⁸ The rate and extent of TTR tetramer dissociation diminished proportional to the concentration of covalent kinetic stabilizer added (Figure 5c). Compound **4** is superior at both stoichiometries employed, likely owing to its high affinity, negatively cooperative binding, and subsequent fast chemoselective reaction kinetics with Lys-15 (recall the 10 min incubation period before adding urea). The negatively cooperative binding minimizes the fraction of unconjugated TTR tetramer by minimizing the fraction of TTR subunits having two covalently attached ligands at a concentration of 1.8 μM . In other words, the negatively cooperative binding maximizes the TTR tetramer population having at least one covalent kinetic stabilizer attached.

Evaluating the Selectivity of Modification of WT-TTR by Covalent Kinetic Stabilizer **4** in Human Blood Plasma

To demonstrate how selective the binding and subsequent chemoselective reaction between **4** and TTR is in human plasma, its ability to covalently modify TTR in human plasma was investigated by quantitative immunoblotting to determine the total TTR concentration in blood plasma and by HPLC to determine the fraction of TTR-(**4**)_n conjugate formed. The

total WT-TTR tetramer concentration in human plasma was established to be $\sim 5.18 \pm 0.34 \mu\text{M}$ (i.e., $20.88 \mu\text{M}$ TTR monomer; $0.29 \pm 0.02 \text{ mg/mL}$) (Figure 6a). To quantify the amount of TTR subunits labeled by covalent kinetic stabilizer **4** in human plasma, we monitored the fluorescence signal of the conjugate using RP-HPLC coupled to a fluorescence detector (FL-RP-HPLC). A standard curve of labeled WT-TTR-(**4**)_n was first generated by FL-RP-HPLC by correlating the amount of labeled TTR injected on the HPLC column with the fluorescence signal peak area (Figure S7). The candidate covalent kinetic stabilizer **4** was subsequently incubated with plasma at two different concentrations, 20 and 40 μM (30 min, 37°C). The TTR subunits in plasma modified by **4** were quantified by integrating the RP-HPLC fluorescence peak area and calculating the concentration from the standard curve (Figures 6b and S7). We observed that 3.6 μM monomeric TTR (0.05 mg/mL) and 5.76 μM monomer TTR (0.08 mg/mL) were labeled when using 20 μM and 40 μM of **4**, respectively, resulting in a modification efficiency of 17% and 28%, respectively, corresponding to 34 and 56% of the tetramers being covalently modified by **4**. Thus, a higher concentration of covalent kinetic stabilizer improves the modification efficiency (Figure 6b, lower panel). Given that analogs of **4** have yet to be prepared to enhance binding affinity and thus lower K_i , it appears that the enhanced electrophilicity of the vinyl sulfonamide can result in a relatively selective and efficient covalent kinetic stabilizer to label TTR in human plasma at the concentrations employed, due to its fast kinetics (k_{chem}). That **4** is a very selective covalent modifier of TTR in *E.coli* lysate (see below) supports our hypothesis that we haven't yet made enough analogs of **4** yet to improve binding selectivity and thus achieve selective TTR conjugate formation in human plasma.

We further probed why increasing the amount of **4** did not react with all of the soluble TTR in human plasma by hypothesizing that **4** could potentially react with endogenous thiol groups of small molecules and proteins due to its intrinsic reactivity as a Michael acceptor. To scrutinize this hypothesis, we first evaluated the selectivity of **4** for labeling TTR in the presence of glutathione (GSH) in buffer. The inherent fluorescence of the conjugate formed from the reaction between TTR and **4** (see below for more details) was employed to monitor conjugate formation kinetics. Compound **4** remains dark when its carbon-carbon double bond is reduced by GSH (Table 2). If **4** were to react efficiently with GSH, a decreased rate of TTR conjugate formation and a decreased final fluorescence amplitude would be observed. However, neither was observed in presence of 10 μM glutathione in nitrogen purged buffer, which is 3 fold higher than the reported mean concentration of GSH in human plasma (Figure S8).³⁸ Thus, a GSH reaction with **4** is likely not responsible for diminishing its efficiency of TTR conjugate formation in human plasma.

An alternative explanation for the inefficient labeling of TTR by **4** in human plasma is that **4** reacts with an additional protein(s). We performed SDS-PAGE of human plasma treated with **4** and imaged the gel using a fluorescence scanner. A significant off-target band was observed in addition to the TTR conjugate band, indicating the inefficiency of TTR labeling by **4** was due in large part to the labeling of another plasma protein (Figure S9). The additional protein reacting with **4** appears to be albumin. The albumin concentration in human plasma is an order of magnitude higher than the concentration of TTR. We hypothesize that through analog synthesis and SAR studies to improve K_i , it is likely that the selectivity of TTR conjugate formation in human plasma could be improved starting with **4**.

Evaluating the Mechanism of the Fluorogenicity of Compound **4**

We have a strong interest in creating “fluorogenic TTR covalent modifiers”, small molecules that remain dark after TTR binding and only become fluorescent upon reaction with TTR.^{23,24,39} We intend to use these fluorogenic compounds as TTR folding sensors and ultimately for cellular imaging applications,^{40,41} as described previously.^{23,24} Thus, we

examined the fluorogenicity of compound **4** and its origins, as well as its conjugation selectivity in samples other than human plasma wherein selectivity needs to be improved.

To test whether **4** is a fluorogenic compound,^{23,24,39} we recorded its fluorescence emission spectra without and with WT- or K15A-TTR added (Figure 7a). No emission was observed from compound **4** alone in buffer, or when **4** is bound to K15A-TTR. In striking contrast, incubation of **4** with WT-TTR for 3 min afforded a conjugate exhibiting maximal emission at 395 nm (excitation at 327 nm). Moreover, the intensity of fluorescence observed at 3 min depended on the amount of **4** added to WT-TTR. Thus, generation of fluorescence appears to require the reaction of **4** with the Lys-15 residue of TTR, suggesting the TTR-**4** conjugation reaction was critical for the emergence of fluorescence. Moreover, the time course of TTR-**4** conjugation monitored by RP-HPLC and the fluorescence emission per unit time at 395 nm in a fluorescence spectrometer were nearly identical (Figure 7b), providing additional evidence that covalent conjugation is required for the emergence of fluorescence. Taken together, the data show that **4** is a fluorogenic small molecule, in that fluorescence only emerges when **4** reacts with WT-TTR.

To further probe the origins of fluorogenicity, we synthesized compound **5** (Table 1), an analogue of **4** incapable of reacting with WT-TTR that simulates the reduced Michael addition product. We measured the quantum yields of compounds **4** and **5** in different solvents in an effort to determine the potential role of the reduction of the double bond (covalent modification), in switching on environmentally sensitive fluorescence. As shown in Table 3 and Figure S10, compound **4** featuring a vinyl sulfonamide functional group is dark in both polar solvents (buffer) and in non-polar solvents (benzene), suggesting that its fluorescence is likely quenched by photoisomerization of the double bond comprising the vinyl sulfonamide substituent.⁴²⁻⁴⁷ Compound **5**, mimicking the conjugate addition product, exhibited no fluorescence in buffer, however it afforded weak fluorescence ($\Phi=15\%$) in benzene, indicating that it is an environmentally sensitive fluorophore, likely owing to the loss of vinyl sulfonamide photoisomerization mentioned above. Binding of **5** in the hydrophobic T₄-binding pocket of WT-TTR doubled the fluorescence intensity ($\Phi=32\%$), but the intensity was still not comparable to that of the WT-TTR conjugate derived from **4** ($\Phi=78\%$), indicating that the binding environment of the chromophore in the TTR•**5** complex and the WT-TTR conjugate derived from **4** are not equivalent. Taken together, all lines of evidence support the hypothesis that covalent modification of TTR by **4** converts a dark compound (**4**) into an environmentally sensitive fluorophore, leading to conjugate fluorescence owing to the placement of the chromophore in the hydrophobic TTR binding pocket. Importantly, the chemoselective reaction between TTR and **4** acts as a fluorogenic switch to eliminate photoisomerization of the stilbene double bond, which is an established mechanism of non-radiative energy dissipation.⁴²⁻⁴⁷

Evaluation of the Kinetics of the Conjugation Reaction by Fluorescence

Having established that **4** is a fluorogenic TTR covalent modifier, we further demonstrated that conjugate fluorescence doubles when 2 rather than 1 of TTRs two binding sites are covalently occupied (Figure S11). We took advantage of this property to quantify the kinetics of the covalent modification of TTR by **4** in buffer. Using a fixed concentration of **4** (0.2 μM) and variable concentrations of TTR to ensure that the TTR binding pockets are in excess (0.25 μM , 1 μM , 2 μM , 4 μM , 15 μM , and 18.5 μM TTR binding pockets; i.e., twice the TTR tetramer concentration employed), we examined the time-dependent emergence of fluorescence upon mixing **4** and WT-TTR in buffer. In all cases, the emergence of fluorescence over time exhibited single exponential kinetics, allowing for calculation of the observed rate constant (k_{obsd}) at each TTR binding pocket concentration (Figure S12). Fitting k_{obsd} vs. TTR binding pocket concentration to a hyperbolic model yielded a $k_{\text{chem}} =$

0.28 min^{-1} (the maximum rate of conjugation) and a $K_1 = 1.2 \text{ }\mu\text{M}$ (concentration of **4** that yields a half maximal rate of conjugation; Figure 8), consistent with the conjugation kinetics measured by FL-RP-HPLC or by conjugate fluorescence assessed in a fluorescence spectrometer (Figure 7b).

The TTR Conjugation Selectivity of **4** is Sufficient to Quantify TTR Concentration in *E.coli* Lysate using a Fluorescence Plate Reader

The conjugate resulting from the reaction between **4** and TTR exhibits the highest fluorescence emission intensity observed to date, 4-fold higher than the TTR-**6** conjugate and 5-fold higher than the TTR-**7** conjugate (Figure 9). The fact that the TTR conjugate derived from **4** exhibits a quantum yield of 78% and the highest fluorescence intensity of all the previously reported TTR fluorogenic probes affords us an opportunity to quantify the concentration of native tetrameric TTR in a complex cellular context.

To determine whether **4** is capable of quantifying the TTR concentration in a complex cellular context, we first scrutinized its conjugation selectivity by following the fluorescence after mixing *E. coli* K12 cell lysate with **4** in the absence of TTR. Notably, compound **4** exhibited no measurable background fluorescence upon adding **4** ($20 \text{ }\mu\text{M}$) into *E. coli* lysate for a period of 50 min (Figure 10a, red curve; $0 \text{ }\mu\text{M}$ TTR). However addition of known TTR concentrations into *E. coli* lysate followed by treatment with **4** ($20 \text{ }\mu\text{M}$) afforded fluorescence amplitudes and kinetics profiles (Figure 10a, red curves) that are nearly identical with those resulting from addition of known recombinant TTR concentrations into buffer treated with **4** ($20 \text{ }\mu\text{M}$; Figure 10a, black curves). The efficiency and accuracy of TTR quantification is not diminished in *E. coli* lysate relative to buffer, even when the stoichiometry of TTR (equivalent to $14.4 \text{ }\mu\text{M}$ binding pockets) approaches that of **4** ($20 \text{ }\mu\text{M}$; a TTR binding pocket : **4** stoichiometry of 1:1.38; Figure 10a, cf. black and red curves at $7.2 \text{ }\mu\text{M}$ TTR). That TTR quantification in lysate by fluorescence correlates well with the TTR standards in buffer (Figure 10b), indicates that **4** is a selective fluorogenic probe that reports on the concentration of native tetrameric TTR in *E. coli* lysates. Lastly, we examined the reaction selectivity of **4** towards the *E. coli* proteome in lysate by SDS-PAGE. Unlike the situation with TTR in human plasma, where **4** reacts with TTR and apparently albumin (Figure S9), no significant off-target band (Figure S13, Lane 5) was observed when lysate without TTR was incubated with **4** ($40 \text{ }\mu\text{M}$). In contrast, added TTR ($3.6 \text{ }\mu\text{M}$) was efficiently labeled by **4** (Figure S13, Lane 6). Although **4** harbors a reactive electrophile, the k_{chem} of **4** coupled with its superior binding selectivity in *E. coli* lysate relative to human plasma allows compound **4** to selectively quantify the concentration of TTR in *E. coli* lysate. The fluorogenicity of **4** coupled with its brightness enables the concentration of folded and properly assembled TTR to be quantified in *E. coli* lysate using a fluorescence plate reader.

CONCLUSIONS

In summary, we have outlined the strategy used to generate a fluorogenic and traceless covalent kinetic stabilizer of TTR. This molecule was shown to be chemoselective towards reaction with the pK_a -perturbed Lys-15 ϵ -amino group of TTR, exhibiting fast reaction kinetics *in vitro* and in *E. coli* lysate. Covalent modification by the kinetic stabilizer **2** or **4** also inhibits dissociation of the TTR tetramer preventing aggregation *in vitro*. In addition, the selectivity and efficiency of **4** for modifying TTR in human plasma is good, although this selectivity needs to be improved by additional medicinal chemistry efforts to evolve **4** into a drug candidate for use in human plasma. Fluorogenic compound **4** very efficiently forms a conjugate with native tetrameric TTR in in *E. coli* lysate, allowing for TTR's rigorous quantification in this complex biological fluid. Given that the *E. coli* proteome and the human plasma are both made up of ≈ 4000 proteins, it stands to reason that with future

structure-activity relationship studies it will be possible to transform **4** into a TTR specific fluorogenic probe to efficiently quantify TTR in human plasma.

Supplementary Material

Refer to Web version on PubMed Central for supplementary material.

Acknowledgments

This work was supported by the National Institutes of Health grant DK046335 (JWK) as well as the Skaggs Institute for Chemical Biology and the Lita Annenberg Hazen Foundation. JCG was supported by a NRSA from the NHLBI (F32-HL099245). We thank the General Clinical Research Center of the Scripps Research Institute for providing human blood. Portions of this research were carried out at the Stanford Synchrotron Radiation Light source, a Directorate of SLAC National Accelerator Laboratory and an Office of Science User Facility operated for the U.S. Department of Energy Office of Science by Stanford University. The SSRL Structural Molecular Biology Program is supported by the DOE Office of Biological and Environmental Research, and by the National Institutes of Health, National Institute of General Medical Sciences (including P41GM103393) and the National Center for Research Resources (P41RR001209).

References

1. Sawaya MR, Sambashivan S, Nelson R, Ivanova MI, Sievers SA, Apostol MI, Thompson MJ, Balbirnie M, Wiltzius JJW, McFarlane HT, Madsen AO, Riekel C, Eisenberg D. *Nature*. 2007; 447:453. [PubMed: 17468747]
2. Chiti F, Stefani M, Taddei N, Ramponi G, Dobson CM. *Nature*. 2003; 424:805. [PubMed: 12917692]
3. Dobson CM. *Nature*. 2003; 426:884. [PubMed: 14685248]
4. Cohen FE, Kelly JW. *Nature*. 2003; 426:905. [PubMed: 14685252]
5. Laganowsky A, Liu C, Sawaya MR, Whitelegge JP, Park J, Zhao M, Pensalfini A, Soriaga AB, Landau M, Teng PK, Cascio D, Glabe C, Eisenberg D. *Science*. 2012; 335:1228. [PubMed: 22403391]
6. Benson MD. *Muscle Nerve*. 2013; 47:157. [PubMed: 23169427]
7. Coelho T, Carvalho M, Saraiva MJ, Alves I, Almeida MR, Costa PPJ. *Rheumatol*. 1993; 20:179.
8. Coelho T, Maia L, Martins da Silva A, Waddington Cruz M, Planté-Bordeneuve V, Lozeron P, Suhr OB, Campistol JM, Conceição I, Schmidt HH-J, Trigo P, Kelly JW, Labaudinière R, Chan J, Packman J, Wilson A, Grogan DR. *Neurology*. 2012; 79:785. [PubMed: 22843282]
9. Coelho T, Maia LF, Martins dSA, Cruz MW, Plante-Bordeneuve V, Suhr OB, Conceicao I, Schmidt HHJ, Trigo P, Kelly JW, Labaudiniere R, Chan J, Packman J, Grogan DR. *J Neurol*. 2013 in press, Ahead of Print.
10. Hammarstrom P, Schneider F, Kelly JW. *Science*. 2001; 293:2459. [PubMed: 11577236]
11. Hammarstrom P, Wiseman RL, Powers ET, Kelly JW. *Science*. 2003; 299:713. [PubMed: 12560553]
12. Herlenius G, Wilczek HE, Larsson M, Ericzon BG. *Transplantation*. 2004; 77:64. [PubMed: 14724437]
13. Sekijima Y, Dendle MA, Kelly JW. *Amyloid*. 2006; 13:236. [PubMed: 17107884]
14. Tojo K, Sekijima Y, Kelly JW, Ikeda S. *Neuroscience Research*. 2006; 56:441. [PubMed: 17028027]
15. Yamashita T, Ando Y, Okamoto S, Misumi Y, Hirahara T, Ueda M, Obayashi K, Nakamura M, Jono H, Shono M, Asonuma K, Inomata Y, Uchino M. *Neurology*. 2012; 78:637. [PubMed: 22345221]
16. Colon W, Kelly JW. *Biochemistry*. 1992; 31:8654. [PubMed: 1390650]
17. Johnson SM, Connelly S, Fearn C, Powers ET, Kelly JW. *J Mol Biol*. 2012; 421:185. [PubMed: 22244854]
18. Hammarstrom P, Jiang X, Hurshman AR, Powers ET, Kelly JW. *Proc Natl Acad Sci USA*. 2002; 99(Suppl 4):16427. [PubMed: 12351683]

19. Foss TR, Kelker MS, Wiseman RL, Wilson IA, Kelly JW. *J Mol Biol.* 2005; 347:841. [PubMed: 15769474]
20. Wiseman RL, Johnson SM, Kelker MS, Foss T, Wilson IA, Kelly JW. *J Am Chem Soc.* 2005; 127:5540. [PubMed: 15826192]
21. Johnson SM, Petrassi HM, Palaninathan SK, Mohamedmohaideen NN, Purkey HE, Nichols C, Chiang KP, Walkup T, Sacchettini JC, Sharpless KB, Kelly JW. *J Med Chem.* 2005; 48:1576. [PubMed: 15743199]
22. Choi S, Connelly S, Reixach N, Wilson IA, Kelly JW. *Nat Chem Biol.* 2010; 6:133. [PubMed: 20081815]
23. Choi S, Ong DS, Kelly JW. *J Am Chem Soc.* 2010; 132:16043. [PubMed: 20964336]
24. Grimster NP, Connelly S, Baranczak A, Dong J, Krasnova LB, Sharpless KB, Powers ET, Wilson IA, Kelly JW. *J Am Chem Soc.* 2013; 135:5656. [PubMed: 23350654]
25. Singh J, Petter RC, Baillie TA, Whitty A. *Nat Rev Drug Discovery.* 2011; 10:307.
26. Klabunde T, Petrassi HM, Oza VB, Raman P, Kelly JW, Sacchettini JC. *Nature structural biology.* 2000; 7:312.
27. Connelly S, Choi S, Johnson SM, Kelly JW, Wilson IA. *Curr Op Sruct Biol.* 2010; 20:54.
28. Choi S, Reixach N, Connelly S, Johnson SM, Wilson IA, Kelly JW. *J Am Chem Soc.* 2010; 132:1359. [PubMed: 20043671]
29. Johnson SM, Connelly S, Wilson IA, Kelly JW. *J Med Chem.* 2008; 51:6348. [PubMed: 18811132]
30. Johnson SM, Connelly S, Wilson IA, Kelly JW. *J Med Chem.* 2008; 51:260. [PubMed: 18095641]
31. Johnson SM, Connelly S, Wilson IA, Kelly JW. *J Med Chem.* 2009; 52:1115. [PubMed: 19191553]
32. Lashuel HA, Lai Z, Kelly JW. *Biochemistry.* 1998; 37:17851. [PubMed: 9922152]
33. Liu S, Hanzlik RP. *J Med Chem.* 1992; 35:1067. [PubMed: 1552501]
34. Jiang X, Smith CS, Petrassi HM, Hammarstrom P, White JT, Sacchettini JC, Kelly JW. *Biochemistry.* 2001; 40:11442. [PubMed: 11560492]
35. Baranczak A, Connelly SP, Liu Y, Choi S, Grimster NP, Powers ET, Wilson IA, Kelly JW. *Biopolymers.* 2013 in press.
36. Lai Z, Colon W, Kelly JW. *Biochemistry.* 1996; 35:6470. [PubMed: 8639594]
37. Hurshman AR, White JT, Powers ET, Kelly JW. *Biochemistry.* 2004; 43:7365. [PubMed: 15182180]
38. Michelet F, Gueguen R, Leroy P, Wellman M, Nicolas A, Siest G. *Clin Chem.* 1995; 41:1509. [PubMed: 7586526]
39. Baranczak A, Connelly SP, Liu Y, Choi S, Grimster NP, Powers ET, Wilson IA, Kelly JW. *Biopolymers.* 2013 in press.
40. Jing C, Cornish VW. *Acc Chem Res.* 2011; 44:784. [PubMed: 21879706]
41. Sun X, Zhang A, Baker B, Sun L, Howard A, Buswell J, Maurel D, Masharina A, Johnsson K, Noren CJ, Xu MQ, Correa IR Jr. *Chembiochem.* 2011; 12:2217. [PubMed: 21793150]
42. Gorner H, Kuhn HJ. *Adv Photochem.* 1995; 19:1.
43. Malkin S, Fischer E. *J Phys Chem.* 1964; 68:1153.
44. Saltiel J. *J Am Chem Soc.* 1967; 89:1036.
45. Saltiel J, Dagostin Jt. *J Am Chem Soc.* 1972; 94:6445.
46. Saltiel J, Marinari A, Chang DWL, Mitchener JC, Megarity ED. *J Am Chem Soc.* 1979; 101:2982.
47. Saltiel J, Zafiriou OC, Megarity ED, Lamola AA. *J Am Chem Soc.* 1968; 90:4759.
48. Wojtczak A, Cody V, Luft JR, Pangborn W. *Acta Crystallogr D Biol Crystallogr.* 1996; 52:758. [PubMed: 15299640]

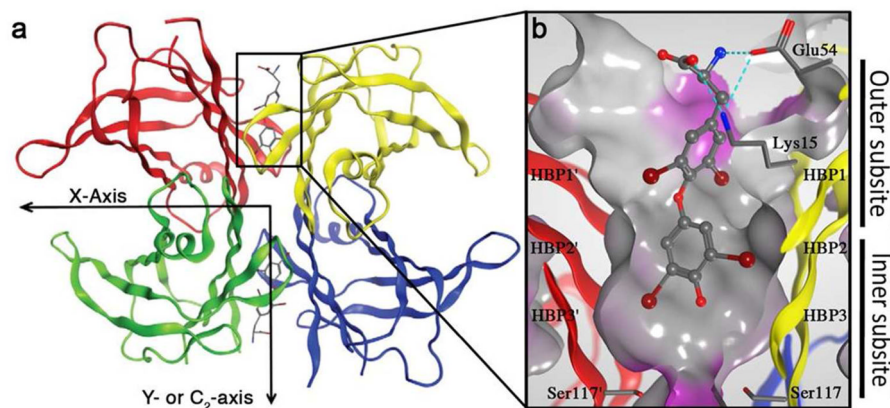


Figure 1.

Structure of tetrameric WT-TTR highlighting the T₄-binding pocket and the pK_a-perturbed Lys15 residue. (a) Crystal structure of WT-TTR in complex with T₄ (PDB accession code 2ROX⁴⁸), depicted in a ribbon format wherein each subunit is colored uniquely (b) Close-up view of one of the two identical T₄-binding sites with a “Connolly” molecular surface applied to residues within 8 Å of T₄ (hydrophobic = grey, polar = purple). The innermost halogen binding pockets (HBPs) 3 and 3' are composed of the methyl and methylene groups of Ser117/117', Thr119/119', and Leu110/110'. HBPs 2 and 2' are made up by the side chains of Leu110/110', Ala109/109', Lys15/15', and Leu17/17'. The outermost HBPs 1 and 1' are lined by the methyl and methylene groups of Lys15/15', Ala108/108', and Thr106/106'. These figures were generated using the program MOE (2011.10), Chemical Computing Group, Montreal, Canada.

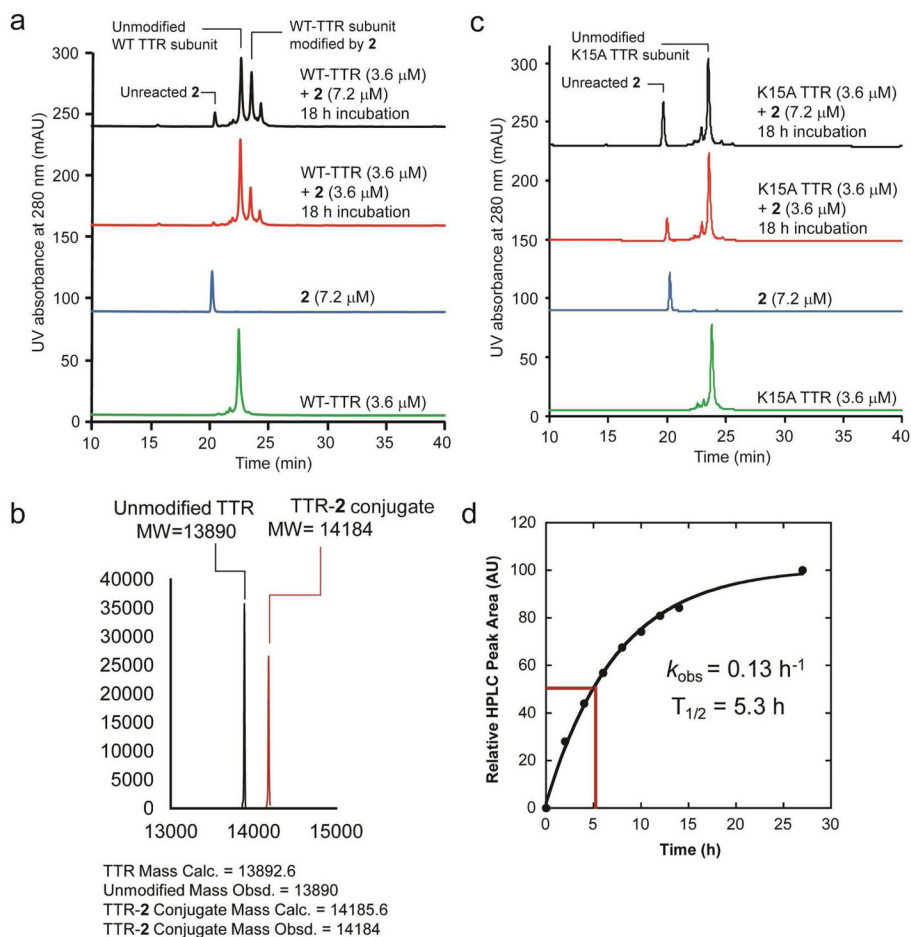


Figure 2. Stilbene-*para*-vinyl amide **2** covalently labels TTR. **(a)** RP-HPLC chromatograms of WT-TTR (3.6 μM) incubated with **2** (7.2 μM or 3.6 μM) showing an additional peak corresponding to the conjugate formed from the reaction between WT-TTR and **2**. **(b)** LC-ESI-MS spectrum of WT-TTR and WT-TTR-**2** conjugate. TTR mass calc. is 13892.6; Unmodified mass obsd. is 13890; TTR-**2** conjugate mass calc. is 14185.6; TTR-**2** conjugate mass obsd. is 14184. **(c)** RP-HPLC chromatograms of K15A-TTR (3.6 μM) incubated with **2** (7.2 μM or 3.6 μM) indicating no modification of K15A-TTR by **2**. **(d)** Time course of the conjugation reaction between WT-TTR (3.6 μM) and **2** (7.2 μM) at 37°C, assessed by integrating the conjugate HPLC peak. The $t_{1/2}$ derived from fitting an exponential to the data is 5.3 h.

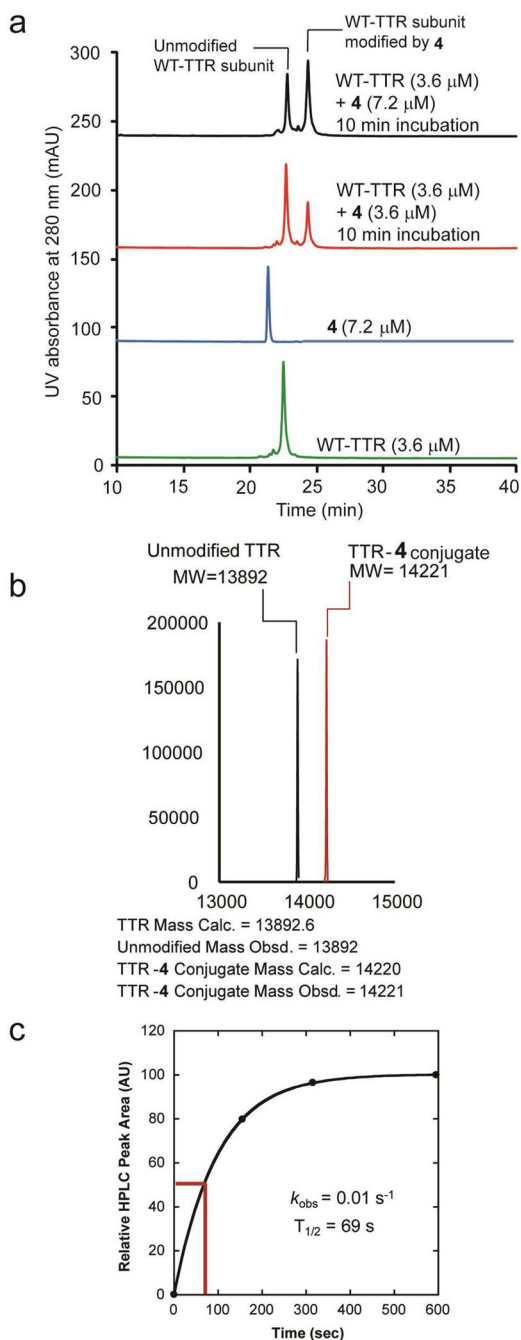


Figure 3.

Vinyl sulfonamide **4**, a more reactive electrophile, covalently labels TTR efficiently in buffer. (a) RP-HPLC chromatograms of WT-TTR (3.6 μ M) incubated with **4** (7.2 μ M or 3.6 μ M) for 10 min at 37 $^{\circ}$ C, showing an additional peak corresponding to WT-TTR subunits modified by **4**. (b) LC-ESI-MS spectrum of WT-TTR and WT-TTR modified by **4**. TTR-**4** conjugate mass calc. is 14220; TTR-**4** conjugate mass obsd. is 14221. (c) Time course of the conjugation reaction between WT-TTR (3.6 μ M) and **4** (7.2 μ M) at 37 $^{\circ}$ C, assessed by integrating the HPLC conjugate peak. The $t_{1/2}$ extracted from fitting an exponential to the data is 69 sec.

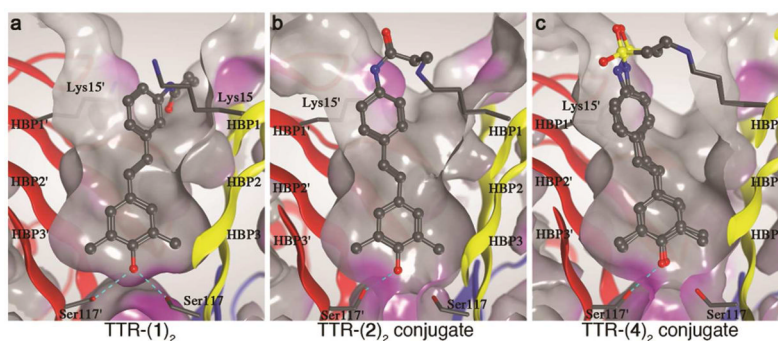
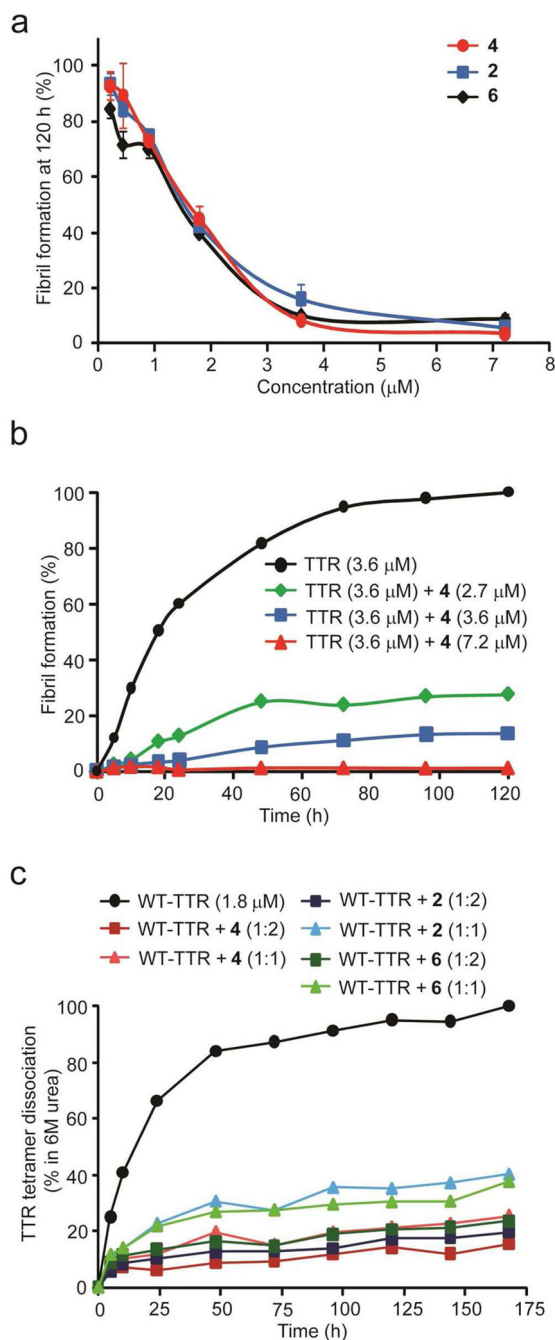


Figure 4.

Crystal structures of homotetrameric WT-TTR in complex with inhibitor **1** and when covalently modified by covalent kinetic stabilizers **2** and **4** (panels a–c, respectively). In each case a close-up view of one of the two identical T₄-binding sites is depicted in a ribbon format wherein each subunit is colored uniquely. A “Connolly” molecular surface was applied to residues within 8 Å of the kinetic stabilizer in the T₄-binding pocket, depicting a hydrophobic surface in gray and a polar surface as purple. The innermost HBPs 3 and 3' are composed of the methyl and methylene groups of Ser117/117', Thr119/119', and Leu110/110'. HBPs 2 and 2' are made up by the side chains of Leu110/110', Ala109/109', Lys15/15', and Leu17/17'. The outermost HBPs 1 and 1' are lined by the methyl and methylene groups of Lys15/15', Ala108/108', and Thr106/106'. Hydrogen bonds shown in light-blue dashed lines. This figure was generated using the program MOE (2011.10).

**Figure 5.**

Covalent kinetic stabilizers inhibit TTR tetramer dissociation and amyloidogenesis. **(a)** Concentration-dependent inhibition of acid-mediated WT-TTR fibril formation by covalent kinetic stabilizers **2**, **4** and **6** (10 min preincubation period at neutral pH) over a 120 h time course after reducing the pH to 4.4 **(b)** Acid-mediated fibril formation was examined at the indicated time points (37°C) as a function of the concentration of compound **4**, pH 4.4–a 10 min preincubation of **4** with WT-TTR at neutral pH was employed **(c)** Urea-mediated (6 M) dissociation and denaturation kinetics of WT-TTR preincubated with compound **2**, **4** and **6**

for 10 min at 37°C. Linked slow dissociation and rapid denaturation were measured by far-UV circular dichroism at 215–218 nm at the indicated time points in 6 M urea.

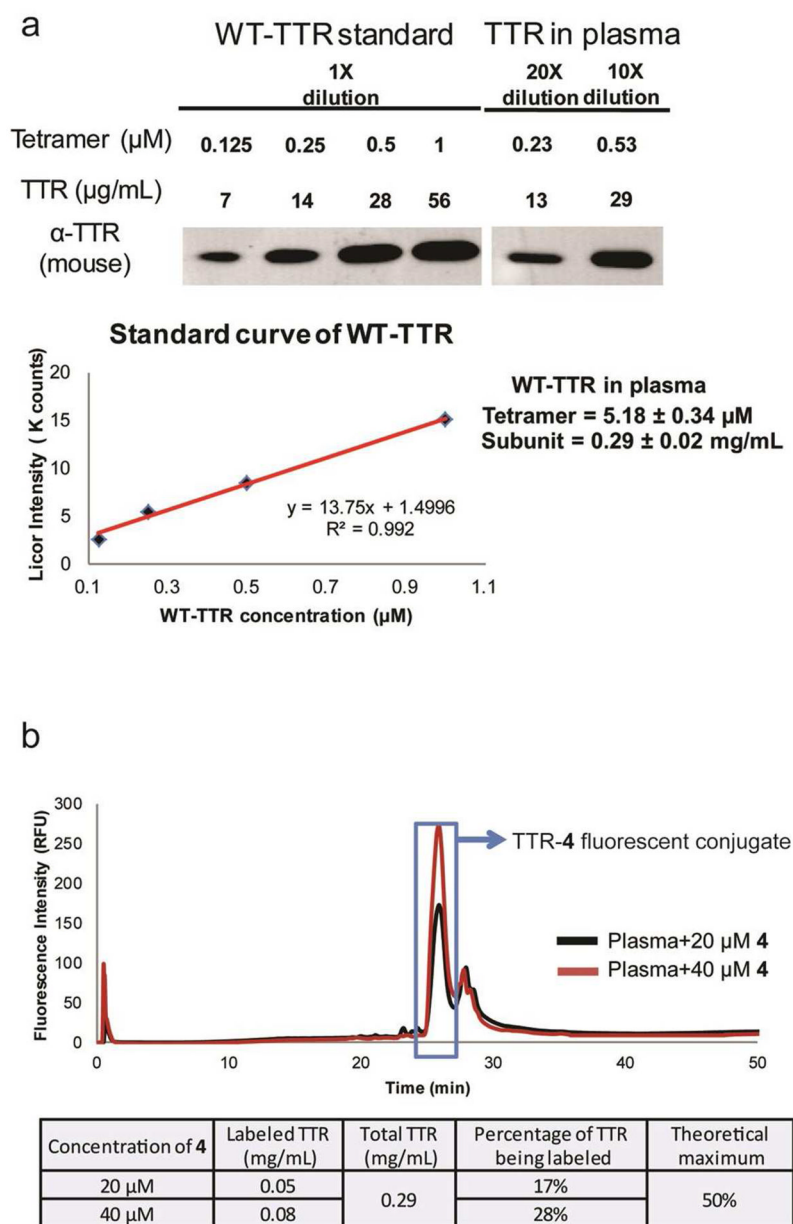


Figure 6. TTR-(4)_n 2 conjugate formation selectivity and yield in human plasma. (a) The concentration of total TTR in human plasma was assessed by quantitative immunoblotting using an immunoblotting standard curve generated from recombinant WT-TTR. (b) Concentration of TTR-4 conjugate formed upon reaction of 4 (20 or 40 μM) with TTR in human plasma is quantified by RP-HPLC employing fluorescence detection $\lambda_{\text{em}} = 395 \text{ nm}$ and a standard curve generated by a reaction between 4 with recombinant TTR (Figure S7). The percentage of modified TTR subunits in human plasma is calculated and summarized, 50% being the maximum, as only 2 of the 4 subunits in the tetramer can be covalently modified by 4.

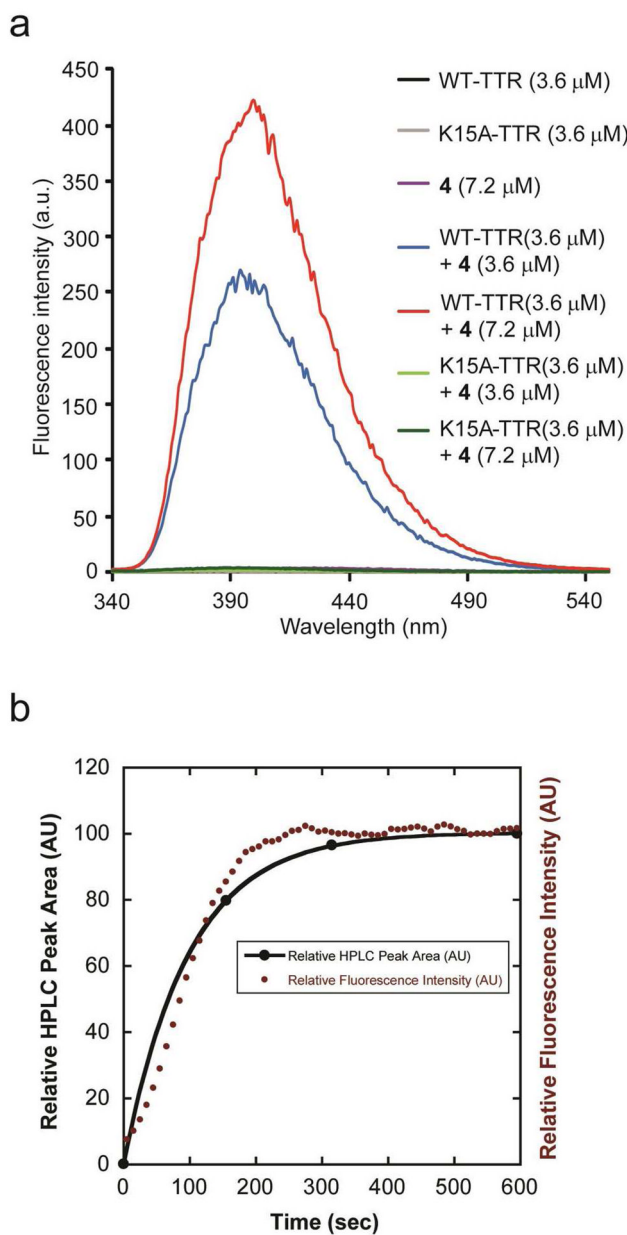


Figure 7. Probing the mechanism of the fluorogenicity of **4**. **(a)** Fluorescence emission spectra of **4** alone, after binding to K15A-TTR, and after binding to and undergoing a conjugation reaction with WT-TTR at 37°C in PBS buffer for 3 min. Excitation $\lambda = 327$ nm, emission max. $\lambda = 395$ nm. **(b)** Overlay of the conjugation time courses derived from WT-TTR (3.6 μ M) reacting with **4** (7.2 μ M) at 37°C assessed by HPLC conjugate peak area (black symbols and curve) and the emergence of conjugate fluorescence in a fluorometer when WT-TTR (3.6 μ M) was incubated with **4** at 37°C in buffer (red trace).

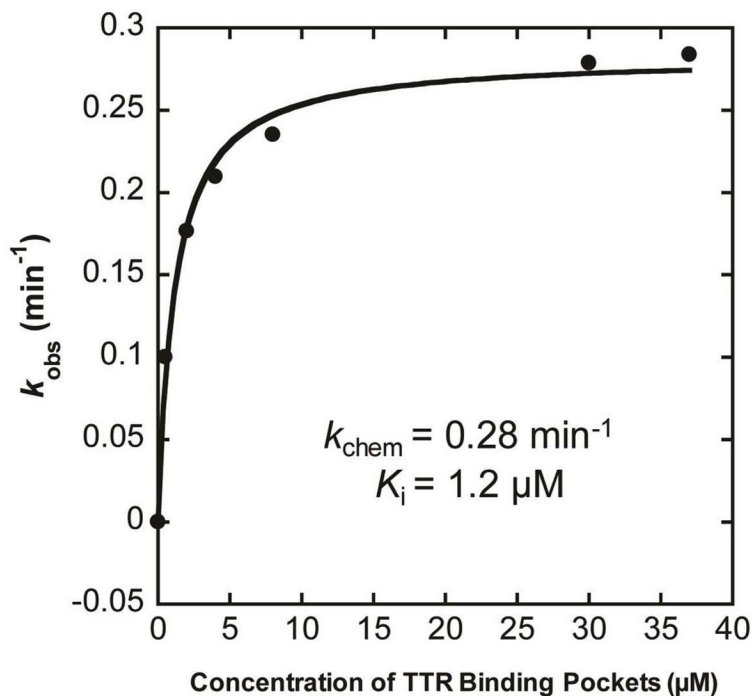


Figure 8.

Kinetics of compound **4** labeling WT-TTR derived from the emergence of conjugate fluorescence in PBS buffer. Compound **4** ($0.2 \mu\text{M}$) was added to increasing concentrations of WT-TTR ($1 \mu\text{M}$ WT-TTR tetramer is equivalent to $2 \mu\text{M}$ binding pockets) in PBS buffer at $25 \text{ }^\circ\text{C}$. Individual k_{obsd} at the different concentrations (Figure S12) were then fitted into a Michaelis-Menten equation. k_{chem} defines the maximum rate of conjugation that is achieved at an infinite concentration of **4**, and K_i defines the concentration of **4** that yields a half maximal rate of conjugation.

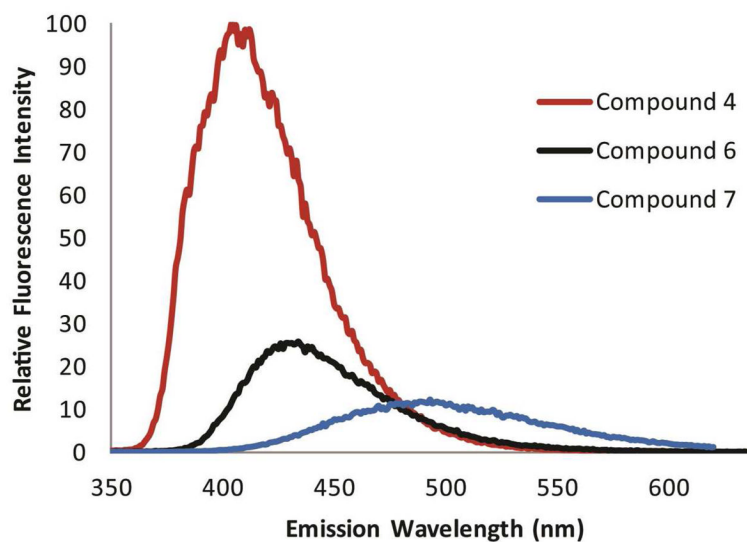


Figure 9.

The conjugate derived from the reaction between compound **4** and WT-TTR exhibits the highest fluorescence intensity of any WT-TTR conjugate prepared to date. Fluorescence emission spectra of the conjugates derived from the reactions of **4**, **6** and **7** with WT-TTR at 37 °C in PBS buffer for 18 h. Excitation λ for **4** = 327 nm, emission max. λ for **4** = 395 nm. Excitation λ for **6** = 328 nm, emission max. λ for **6** = 430 nm. Excitation λ for **7** = 365 nm, emission max. λ for **7** = 520 nm.

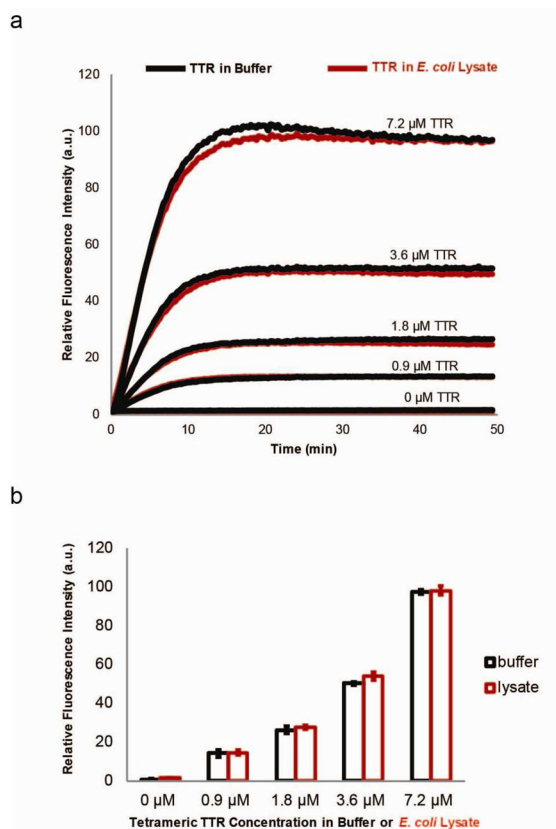


Figure 10.

The selectivity of conjugate formation resulting from the reaction between WT-TTR and **4** is sufficient to quantify the TTR concentration in *E. coli* lysate by fluorescence employing a fluorescence plate reader. (a) Time courses of fluorescent conjugate formation in PBS buffer and in *E. coli* lysate are identical, except at the highest concentration of TTR used where the number of TTR binding sites nearly equals the concentration of **4** employed, where the rate is only slightly faster in buffer. The amplitudes of the fluorescence at the end of the conjugation reaction are identical in *E. coli* lysate and in PBS buffer at all concentrations employed. The indicated concentration of tetrameric TTR was added to *E. coli* lysate or buffer, and subsequently 20 μM **4** was added at 25°C for the indicated time course. (b) Quantification of the fluorescence intensity averaged over the time course from 30–50 min in *E. coli* lysate (in red) correlates well with the intensity averaged over the time course from 30–50 min in buffer (in black), indicating **4** is selective enough to probe the concentration of TTR in *E. coli* lysate. The error bars reflect the standard deviations between 3 biological replicates of this experiment.

Table 1

Structures of compounds synthesized and designed to covalently modify TTR.

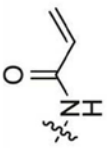
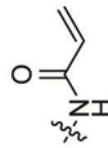
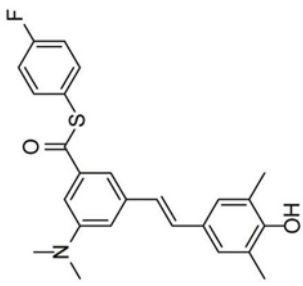
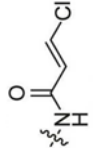
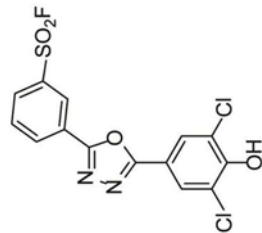
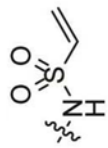
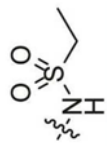
Compound	R	Position	Controls
1		<i>meta</i>	
2		<i>para</i>	
3		<i>para</i>	
4		<i>para</i>	
5		<i>para</i>	

Table 2

Percent fibril formation of WT-TTR (3.6 μ M, pH 4.4) preincubated with compounds **1–4** (3.6 μ M, 7.2 μ M) for 10 min (red font) and 18 h (black font), examined after incubation for 72 h at 37 °C.

	Fibril formation	
	3.6 μ M	7.2 μ M
1	30.1% (\pm 1.7%)	3.0% (\pm 0.2%)
2	16.2% (\pm 5.0%)	6.0% (\pm 0.2%)
	3.8% (\pm 0.5%)	3.5% (\pm 0.1%)
3	23.6% (\pm 1.7%)	4.1% (\pm 0.6%)
4	8.3% (\pm 0.8%)	3.7% (\pm 0.7%)
	7.6% (\pm 1.6%)	3.5% (\pm 0.3%)

Table 3Quantum yields of 4 & 5 under identical incubation conditions.^a

Quantum Yield	TTR	Buffer	Benzene
4	78%±1	0	0
5	32%±4	0	15%±2

^aSee experimental section